# ON THE IGNITION AND COMBUSTION VARIANCES OF JET PROPELLANT-8 AND DIESEL FUEL IN MILITARY DIESEL ENGINES

Peter Schihl* and Laura Hoogterp
RDECOM-TARDEC
Warren, MI. 48397-5000

## ABSTRACT

Currently, the U.S. Army can not purchase commercial off the shelf (COTS) on-road diesel engines for tactical wheeled vehicles due to a variety of reasons related to Environmental Protection Agency (EPA) emission regulations. Such reasons include Jet Propellant-8 (JP-8) incompatibility issues with exhaust aftertreatment devices and cooled exhaust gas recirculation (EGR) systems, unstable combustion regimes at part-load operation while operating on widely varying cetane number fuels such as JP-8, thermal management load increases that impact vehicle mobility and survivability, and high pressure fuel system reliability issues associated with using low lubricity fuels such as JP-8. This submission will briefly discuss these practical engine system issues and then present recent applied research that has focused on quantifying ignition and combustion differences between representative JP-8 and DF-2 samples in direct and indirect injected diesel engines through single and multi-cylinder experimentation, constant volume bomb experiments, spray and liquid length evaporation modeling, and shock tube experiments. The ultimate goal of this effort is to aid military engine suppliers in either converting current COTS engines to operate on JP-8 or in developing the next generation of military engines that must operate on JP-8. Such research is strictly applicable to the Army and other service agencies since military engine suppliers are currently focused on meeting future EPA emission standards which must operate on commercial ultra low sulfur diesel fuel.

## INTRODUCTION

Current on-road diesel engines include cooled EGR, an oxidation catalyst, and a catalyzed diesel particulate filter (CDPF) as part of the emissions control system for meeting nitrous oxide and particulate matter EPA standards. Cooled EGR typically leads to an additional demand on the vehicle thermal management system that requires additional cooling capacity up to 50% in comparison to engines sold in the late 1990's. Such cooling demands are difficult to integrate into a military truck thermal management system without increasing both radiator size and cooling fan power requirement which present potential survivability issues if additional heat exchangers are required to meet such thermal management demands and also lead to higher parasitic fan losses that may impact vehicle mobility. Additionally, high sulfur fuel degrades the durability and reliability of the EGR system, the valves, the valve seats, the piston rings, and the liners due to the formation of sulfuric acid within the EGR and intake system. This issue has been addressed in commercial truck applications by the utilization of ultra low sulfur diesel fuel and new lubricating oil formulations.

Oxidation catalysts are employed in commercial diesel engines in order to convert fuel introduced in the exhaust system into an isotherm utilized to incinerate particulate matter trapped on the CDPF. Fuel sulfur contaminates the oxidation catalyst and thus degrades the conversion performance of this device which can result in fuel slippage through the catalyst in some cases or possibly 'over fueling' of the catalyst in an extreme situation. Both of these scenarios can lead to prolonged high temperature operation of the CDPF and thus is a vehicle signature and safety concern. CDPFs are also sensitive to fuel sulfur since this specie does contaminate active catalytic sites which ultimately leads to longer incineration time periods and potentially higher temperature operation. In additional to high sulfur fuel issues, CDPF's become clogged with continual exposure to ash from lubricant oil and thus require a maintenance schedule for removal and cleaning after a certain period of time. Last, this device presents a survivability issue during incineration events since its operating temperature is on the order of 1000 F.

Current Army policy is to avoid purchasing such engines and instead opt for either off-road engines or earlier model year on-road engines that will meet vehicle mobility and cooling requirements.

These current and future engine systems are and will be utilizing non-standard combustion strategies including low temperature combustion (LTC), premixed charge compression ignition (PCCI), and homogeneous charge compression ignition (HCCI) in order to reduce the amount of nitrous oxide and particulate matter produced in the combustion chamber. These three types of highly premixed combustion and high EGR strategies are sensitive to the ignition quality and evaporation characteristics of the fuel, and thus large variances in the

# Report Documentation Page

*Form Approved*
*OMB No. 0704-0188*



| 1. REPORT DATE | 2. REPORT TYPE | 3. DATES COVERED |
|---|---|---|
| **22 SEP 2008** | **N/A** | **-** |

| 4. TITLE AND SUBTITLE | 5a. CONTRACT NUMBER |
|---|---|
| **On the Ignition and Combustion Variances of Jet Propellant-8 and Diesel Fuel in Military Diesel Engins** | 5b. GRANT NUMBER |
| | 5c. PROGRAM ELEMENT NUMBER |
| 6. AUTHOR(S) | 5d. PROJECT NUMBER |
| **Peter Schihl; Laura Hoogterp** | 5e. TASK NUMBER |
| | 5f. WORK UNIT NUMBER |
| 7. PERFORMING ORGANIZATION NAME(S) AND ADDRESS(ES) | 8. PERFORMING ORGANIZATION REPORT NUMBER |
| **US Army RDECOM-TARDEC 6501 E 11 Mile Rd Warren, MI 48397-5000** | **19172RC** |
| 9. SPONSORING/MONITORING AGENCY NAME(S) AND ADDRESS(ES) | 10. SPONSOR/MONITOR'S ACRONYM(S) |
| **US Army RDECOM-TARDEC 6501 E 11 Mile Rd Warren, MI 48397-5000** | **TACOM/TARDEC** |
| | 11. SPONSOR/MONITOR'S REPORT NUMBER(S) **19172RC** |

12. DISTRIBUTION/AVAILABILITY STATEMENT
**Approved for public release, distribution unlimited**

13. SUPPLEMENTARY NOTES
**Presented at the 26th Army Science Conference, Orlando, Florida, December 2008, The original document contains color images.**

14. ABSTRACT

15. SUBJECT TERMS

| 16. SECURITY CLASSIFICATION OF: | | | 17. LIMITATION OF ABSTRACT | 18. NUMBER OF PAGES | 19a. NAME OF RESPONSIBLE PERSON |
|---|---|---|---|---|---|
| a. REPORT | b. ABSTRACT | c. THIS PAGE | | | |
| **unclassified** | **unclassified** | **unclassified** | **SAR** | **8** | |

cetane number (CN) and 90% distillation temperature present potential major combustion instability issues for such engines. Commercial diesel fuel has a much narrower cetane number variance in North America in comparison to JP-8 as outlined in the 2006 Petroleum Quality Information System (PQIS) report that revealed a JP-8 cetane index variance of 31.8 to 56 with a mean value of 43.4; diesel engine manufacturers typically do not design combustion systems that are normally robust to handle such variances in modern engines. Furthermore, U.S. Army engine suppliers typically design their products for North American or European diesel fuel since both commercial markets are much larger in comparison to military sales volume. It is apparent that engineering models are needed to both assess the impact of JP-8 on such modern combustion systems and also to aid in the design of future specialty military engines for avoiding any unintended combustion instability issues in the mid to long term future. This submission highlights a portion of current internal and external TARDEC research toward developing such engineering models.

## 1. EXPERIMENTAL DIESEL ENGINES

The engine predominately utilized in this study was an AVL 521, single cylinder, high output diesel as shown in table 1 while a second production multi-cylinder turbo-diesel engine also provided supplemental ignition data. A low-pressure, oil-based common rail injection system was integrated into the base AVL 521 engine design through modification of the injector sleeve and valve cover. The original aluminum piston was ground below the second compression ring and retrofitted with a bolt-on steel crown. As a result of this change in reciprocating mass, the crankshaft was rebalanced to provide the necessary operating speed range. Both the coolant and lubrication systems were externally controlled to provide desired flow rate and supply temperature through necessary heat exchangers and valves. Each engine was equipped with piezo-electric or piezo-resistive high pressure sensors to measure combustion chamber pressure in real time.

A low speed data acquisition system application was utilized to collect and process numerous low speed temperature and pressure measurements, and analog output from various flow meters associated with fuel and air consumption, coolant flow rate, and lube oil flow rate. High-speed instrumentation included injector needle lift, oil rail pressure, injection command pulse, driver current, and in-cylinder pressure. Each of these signals was collected using a sixteen (16) channel high speed data acquisition system through crankshaft triggering from a 1440 count optical encoder.

### 1.1 Fuel Injection System

The AVL 521 original base engine included a Bosch PLN (pump-line-nozzle) injection system that had a maximum peak pressure of 700 Bar and variable start of injection capability. This PLN system was replaced with a HEUI-type (hydraulically actuated electronically controlled unit injector) fuel injection system developed by Indiana Research Institute (IRI). The injector was modified to allow for peak injection pressures near 1900 bar at a peak injection quantity of 240 $mm^3$/stroke, and a prototype driver was developed to provide multiple injection capability with minimum dwell times near 0.5 milliseconds and minimum quantities of 10 $mm^3$/stroke. A linear displacement, ring-type transducer was integrated into the injector needle button in order to provide direct real-time needle lift behavior. Fuel system control was provided by a custom built combination low and high speed engine control cart.

**Table 1: Research Engine Specifications**

| Engine Parameter | AVL 521 | GEP 6.5L |
|---|---|---|
| Injection system | Indiana Research Institute BETA | Pump line nozzle (PLN) |
| Max Mean Injection pressure (bar) | 1600 | 700 |
| Nozzle geometry (mm) | Variable | single hole |
| Bore x stroke (mm) | 120 x 120 | 103 x 97 |
| Peak firing pressure (bar) | 200 | 104 |
| Compression ratio (nominal) | 13.7 | 20.2 |
| Swirl number | 1 – 3 | NA |
| Displacement (cc) | 1357 | 6468 |
| Operating speeds (rpm) | 800 – 3000 | 1500 – 3400 |
| IMEP range (bar) | 5 – 27 | 2 – 10 |
| Boost system | Shop air | Turbocharger |

In order to indirectly determine on-engine injection pressure and rate, a test stand was developed to directly measure injection pressure in a simulated engine environment. Nozzle test specimens were modified to interface with a fuel pressure measurement cavity that included necessary sealing, drainage, and a piezo-resistive transducer. This test stand was employed to assess nozzle flow rates, peak injection pressure, and average injection pressure for both properly matching nozzles to the engine and also for ensuring safe on-engine operation given the 1900 bar peak injection pressure limitation on the injector assembly. Two production type nozzles were included in this study for investigating possible mixing effects on the ignition and subsequent heat release events.

### 1.2 Combustion Analysis

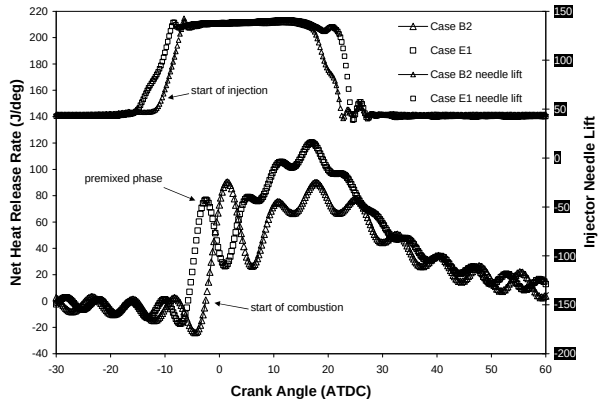


Figure 1: Representative injector needle lift and net heat release rate profiles from the AVL 521.

In-cylinder pressure data was analyzed using TARDEC in-house combustion analysis software called NETHEAT. Essentially, the first law of thermodynamics was applied to a control volume that included the entire combustion chamber throughout the compression and expansion strokes as shown below:

$$\frac{dQ}{d\theta} = \frac{k}{k-1} P \frac{dV}{d\theta} + \frac{1}{k-1} V \frac{dP}{d\theta} \qquad \textbf{(1)}$$

where Q is the net heat release rate (combustion rate less the wall heat transfer rate), k is the specific heat ratio, P is the combustion chamber pressure, V is the combustion chamber volume, and Θ is the crankshaft rotation angle. For the pre-chamber GEP engine, equation (1) was applied to each combustion chamber and then both governing equations were added together to generate the overall net heat release rate based on a single zone, bulk temperature. In order to more accurately estimate the bulk specific heat ratio, a compressibility correction was utilized to correct the bulk temperature (Kanimoto et al., 1997) as given by:

$$\nu = \frac{RT}{P} + 1.09059\, x10^{-3} - \frac{8.50053x10^{-3}}{(T/100)^{1.64}} + \qquad \textbf{(2)}$$

$$\frac{4.34248x10^{-10}}{(T/100)^{2.49}} P - \frac{6.52579x10^{-18}}{(T/100)^{2.92}} P^2 + \frac{2.95689x10^{-26}}{(T/100)^{3.17}} P^3$$

where R is the gas constant. Each combustion chamber specie mole fraction was initialized at a chosen time following intake valve closure and a single step global $C_nH_m$ chemistry model was utilized to determine perturbations in the specie mole fractions upon initiation of the injection process. Since the net apparent heat release rate does not differentiate between heat transfer and gross burning rate, and typical combustion efficiencies in diesel engines are 99%, a speed up factor was incorporated within the chemistry model to ensure a nearly complete burn and thus a more accurate calculation of the charge specific heat ratio. All experimental pressure traces were conditioned with a digital low pass filter that had a cutoff frequency of typically once the engine speed preceding heat release analysis.

An illustrative example of measured needle lift and net heat release rate profiles is given in figure 1. The ignition delay was determined by the difference between the zero cross-over point of the latter and the 15% opening point of the needle based on experience with the nozzle test stand.

Last, numerous experiments were conducted utilizing the AVL 521 engine to generate a database that highlights ignition and combustion variances between DF-2 and JP-8 over a range of ignition temperatures and pressures relevant to military diesel engines. The experimental matrix is given in table 2.

**Table 2: AVL 521 Test Matrix**

| Test Sequence | TIM (EC) | MAP (bar) | SOI (ATDC) | Oil Rail Pressure (bar) |
|---|---|---|---|---|
| A | 66 | 1.7 | -15 to 0 | 207 |
| B | 66 | 2.0 | -15 to 0 | 207 |
| C | 66 | 2.25 | -15 to 0 | 262 |
| D | 77 | 2.0 | -15 to 0 | 262 |
| E | 77 | 2.25 | -15 to 0 | 289 |
| F | 77 | 2.52 | -15 to 0 | 289 |
| G | 88 | 2.52 | -15 to 0 | 289 |
| H | 88 | 2.80 | -15 to 0 | 289 |

TIM: intake manifold temperature; MAP: intake manifold absolute pressure; SOI: start of injection, varied in 3E increments from -15 to 0; ATDC: after top dead center; all experiments conducted at 2500 RPM.

## 2. EVAPORATION AND SPRAY MODELING

The evaporation process in a diesel jet under the constraint that ignition occurs during the injection event can be modeled as a steady-state jet. In this case, the evaporation rate is mixing controlled under the assumption of a finely atomized spray with an advantageous surface area to volume ratio thus promoting a saturated state at the bulk break-up length of the jet (Siebers, 1999). Additionally, this model is based on the judicious selection of a single pure hydrocarbon fuel surrogate that is deemed to properly simulate the real world fuel's evaporation characteristics. This model was further extrapolated to include a method for superposition of dodecane, tetradecane, and hexadecane that adequately simulates JP-8 type fuel evaporation characteristics (Schihl et al., 2006). For completeness, the model is given below and is based on applying the conservation of mass, momentum, and energy to a rectangular control volume that encompasses a propagating conical fuel jet whose tip has reached the saturated state condition:

$$L_b = \frac{b}{a} \sqrt{\frac{\rho_f}{\rho_a}} \frac{\sqrt{C_a} \bullet d}{\tan(\frac{\theta}{2})} \sqrt{\left(\frac{2}{B_s} + 1\right)^2 - 1} \qquad \textbf{(3)}$$

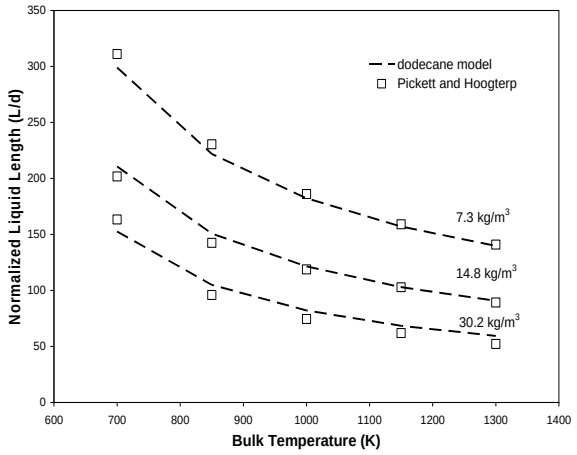


Figure 2: Comparison of JP-8 evaporation bomb data and a dodecane surrogate model.

where a and b are constants, $\rho_f$ is the liquid fuel density, $\rho_a$ is the ambient density, $C_a$ is the nozzle area coefficient, $\theta$ is the spray formation angle, d is the orifice diameter, and $B_s$ is the fuel to ambient gas flow rate ratio or evaporation coefficient. Furthermore, this latter constant $B_s$ is fuel dependent and based on the iterative solution of the conservation of mass and energy. For completeness this relationship is shown below:

$$B_s = \frac{Z_a(T_a, P_a - P_s) \bullet P_a \bullet M_f}{Z_f(T_s, P_s) \bullet (P_a - P_s) \bullet M_a} = \frac{h_a(T_a, P_a) - h_a(T_s, P_a - P_s)}{h_f(T_s) - h_f(T_f, P_a)} \quad \textbf{(4)}$$

where $Z_a$ and $Z_f$ are the ambient and fuel vapor compressibility, $T_f$ is the injected liquid fuel temperature, $T_a$ and $P_a$ are the ambient temperature and pressure, $M_f$ and $M_a$ are the fuel and ambient molecular weights, $T_s$ and $P_s$ are the fuel saturation temperature and pressure, $h_a$ is the ambient enthalpy, and $h_f$ is the fuel enthalpy. For this study, dodecane was employed as a surrogate for JP-8 and hexadecane for DF-2 based on previous modeling efforts (Schihl and Hoogterp, 2006) and experimental studies (Pickett and Hoogterp, 2008) that demonstrated the scientific merit of this choice – see figure 2.

## 3. EXPERIMENTAL RESULTS

Three experimental apparatuses were utilized for this submission – the single cylinder research engine, a constant volume bomb, and a shock tube. The most former was previously discussed in this submission while details of the latter two are readily available from Sandia National Laboratory (Pickett and Hoogterp, 2008) and Stanford University (Vasu et al., 2008). Essentially, the latter two employed shadowgraph imaging, Mie scattering, a photo-detector, and high pressure

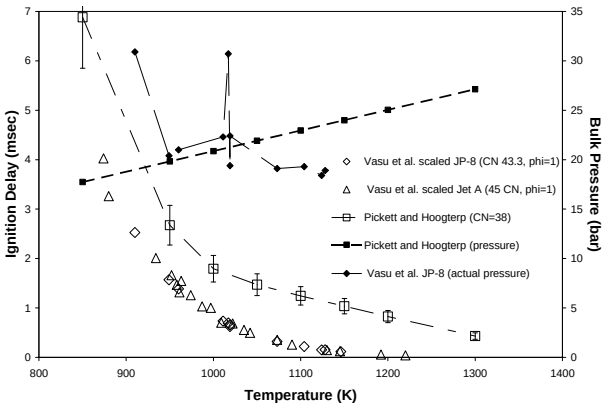


Figure 3: Comparison of JP-8 shock tube and constant volume bomb data at a charge density of 7.27 kg/m$^3$.

measurements to directly and indirectly measure the ignition delay period, the liquid length, and spray formation process. The single cylinder research engine was also utilized to indirectly measure the ignition delay period and the net heat release rate profile through in-cylinder pressure and needle lift measurements. The ensuing discussion will compare and contrast measurements taken from each apparatus in order to further understand any physicochemical induced perturbations in combustion characteristics between DF-2 and JP-8.

### 3.1 Shock Tube and Bomb Ignition Behavior

Jet-A and JP-8 from two different sources were investigated at equivalence ratios of unity and one-half over a range of bulk temperatures indicative of a modern diesel engine with the limitation that the bulk pressure range was limited by the reflected shock measurement technique (Vasu et al, 2008). Nevertheless, such measurements are valuable for assessing JP-8 autoignition chemistry models and also in aiding to understand observed ignition behavior in the single cylinder research engine. For example, a dozen ignition measurements were taken for JP-8 (43.3 CN) over a temperature and pressure range that corresponded to nearly a constant charge density. Such data points were compared to measurements taken in a constant volume bomb (Pickett and Hoogterp, 2008) assuming that the ignition delay scaled inversely with pressure. This latter assumption is reasonable if the resultant scaled pressure did not dramatically vary. As shown in figure 3, the shock tube data exhibited a rapid decrease in the ignition time as the bulk temperature exceeded 1000 K at the given iso-density that corresponded to a bulk pressure ranging from 18 to 32 bar at stoichiometry. This same behavior was also observed for Jet-A (45.3 CN) utilizing the same inverse pressure scaling method. The constant volume bomb data (38 CN) exhibited a similar trend, but never did or will reach zero due to break-up, evaporation, and mixing sub-processes

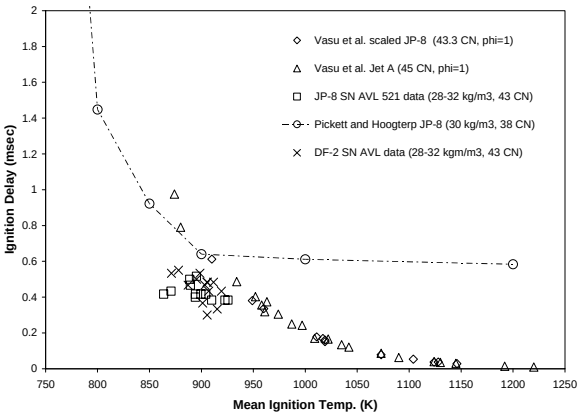


Figure 4: Comparison of JP-8 shock tube, constant volume bomb, and AVL 521 data at a representative light to medium load engine operating condition. Note SN is the small nozzle (0.176 mm).

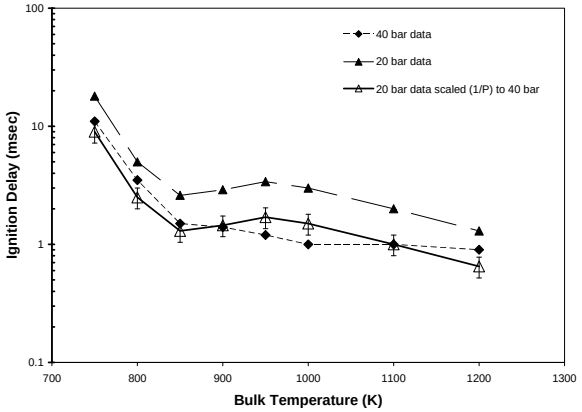


Figure 5: Influence of ignition pressure on the ignition delay of n-heptane in a constant volume bomb.

that precede the onset of pre-ignition chemistry. Therefore, the difference in ignition timing between the shock tube and the constant volume data is a strong function of the jet liquid length (evaporation), injection velocity and nozzle size (break-up and mixing), and cetane number differences (ignition chemistry).

An attempt was also made to scale the shock tube data to an iso-density indicative of a light to medium load condition in a diesel engine as shown in figure 4. The shock tube scaled data rapidly approaches the constant volume bomb data as the bulk temperature decreases toward 900 K and eventually both the AVL 521 engine data (43 CN) and the bomb data (38 CN) exhibit shorter ignition delays in comparison to the shock tube data. This trend is not possible since shock tube ignition data is predominately pure autoignition chemistry while the bomb and engine data involve break-up, evaporation, and mixing sub-processes that are finite in time. This trend points toward the conclusion that the inverse pressure scaling is not valid over the entire temperature range. This point is further demonstrated by studying n-heptane (55 CN) bomb ignition data (Ishiyama et al., 2003) as shown in figure 5. It is clear that the inverse pressure scaling is only valid in the vicinity of 900 K and 1100 K and that a scaling of $P^n$ involves an n that varies from 1 to 1.6 as a function of temperature over this range of interest while n is less than unity above 1100 K and below 900 K. This scaling is also affected by the injection process which would tend to further impact the n value as the injection velocity increases. The n-heptane study was conducted at an average injection velocity on the order of 100 m/s (Ishiyama et al., 2003) while the Sandia bomb data was 500 m/s (Pickett and Hoogterp, 2008), and the engine data was approximately 200 m/s; the exact impact on n is not quantified at this time and will require additional experimental and chemical kinetics modeling efforts.

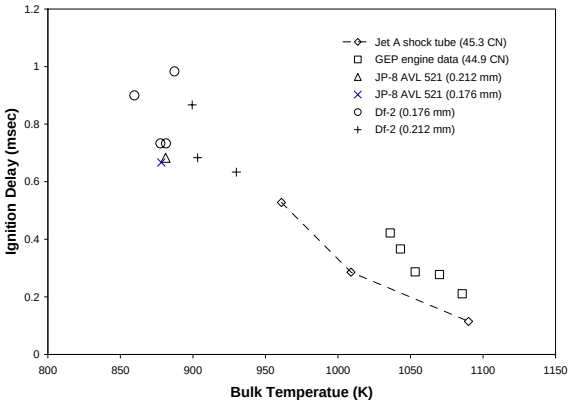


Figure 6: Comparison of JP-8 shock tube and engine data ignition delay data at a charge density of 18 kg/m$^3$.

Most of the shock tube data set did not scale well with typical engine boundary conditions though three Jet-A data points were similar to measurements taken in the AVL 521 and GEP 6.5L turbo-diesel. These various comparable points are shown in figure 6 at a bulk density of approximately 18 kg/m$^3$. The only conclusion that can be drawn from this data set is that the turbulent mixing, high wall temperatures, and 'rich' ignition in the GEP 6.5L turbo-diesel pre-chamber lead to much shorter physical time scales in comparison to the bomb data (see figure 3) and thus much smaller differences in ignition delay between the shock tube and engine data sets. This observation is anticipated since pre-chamber engines historically are less sensitive to cetane number due to their higher pre-injection temperatures and pressures, much higher wall temperatures, and augmented turbulent mixing in comparison to a direct injected diesel engine.

### 3.2 Generalized Engine Ignition Behavior

In general terms, the ignition data generated from the two diesel engines was very comparable to the bomb measurements. As shown in figure 7 at a bulk density of 30 kg/m$^3$, the observed ignition delay in the AVL 521 engine is between 20 to 50% faster than bomb data. This trend is in agreement with the cetane number variance between the bomb data (38 CN) and the AVL 521 engine data (43 CN) as observed in recent bomb experiments highlighting ignition differences between a regional JP-8 (38 CN) and DF-2 (46 CN) that exhibited a 25 to 50% variance (Pickett and Hoogterp, 2008). Additionally, research by various sources (McMillan et al., 1983; Hardenburg and Hase, 1979; Xia and Flanagan, 1987; Teng et al., 2003; Shipinski et al., 1970) has shown that a ten point reduction in cetane number results in approximately a 30% increase in the ignition delay period which partially agrees with the trend demonstrated in this study. Thus, though the variance between the bomb data and AVL 521 engine data is predominately explained by ignition chemistry differences (i.e. cetane number), it is important to note that mixing plays a secondary role since bomb experiments were conducted with an injection velocity of approximately 500 m/s (0.180 mm hole size) while the engine experiments were generally near 200 m/s (0.176 mm hole size). This point is further supported by observing that the AVL 521 large nozzle data sets (0.212 mm) for both JP-8 and DF-2 had on average a 0.1 to 0.15 msec increase in ignition delay in comparison to the small nozzle (0.176 mm) as shown in figure 8.

Additionally, the GEP 6.5L turbo-diesel JP-8 data (44.9 CN) at 24 kg/m$^3$ was also compared with AVL 521 engine and bomb data – see figure 7. It is important to note that the high compression ratio of this pre-chamber engine results in much higher ignition temperatures in comparison to the AVL 521 engine which leads to much shorter ignition delay periods. Previously discussed Jet-A and JP-8 shock tube data demonstrated that the ignition delay period decreased very rapidly after 1000 K and approached zero near 1100 K at bulk pressures of approximately 20 bar. All the GEP engine data shown in figure 7 had mean ignition pre-chamber pressures that ranged from 50 to 90 bar and thus it is anticipated that such higher pressures would reduce the already short ignition delay periods observed in the shock tube by possibly a factor of two based on n-heptane bomb experiments (Ishiyama et al., 2003) and reduced kinetics modeling (Schreiber et al., 1994). Therefore, the bulk of the ignition delay observed in the GEP engine must be dominated by the break-up and mixing processes which is somewhat intuitive since the injector nozzle is a pintle-type with a single hole on the order of 1 mm that has injection velocities of approximately 50 m/s and high velocity entry flow through the prechamber inlet nozzle that leads to augmented turbulent mixing. This type of trend is also in agreement with bomb experiments that

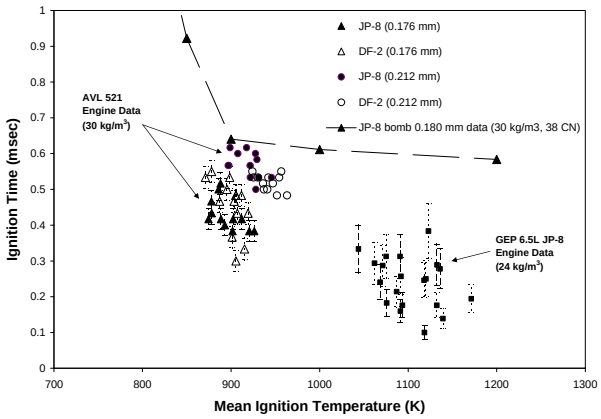


Figure 7: Comparison of JP-8 bomb data and AVL 521 engine data at a charge density of 30 kg/m$^3$. The GEP 6.5L data is presented at a charge density of 24 kg/m$^3$. (Nozzle size is given in the legend.)

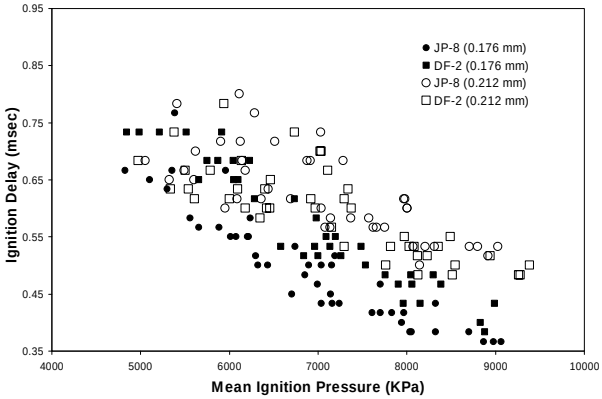


Figure 8: The influence of nozzle hole size on JP-8 and DF-2 ignition delay in the AVL 521.

covered a range of cetane numbers varying from 15 to 100 at a bulk pressure of 30 bar (Siebers, 1985).

### 3.3 Fuel and Nozzle Impact on Ignition

The AVL 521 experiments included utilization of large (0.212 mm) and small (0.176 mm) nozzles for studying mixing variances on ignition and general combustion behavior of JP-8 and DF-2. As shown in figure 8, the small nozzle data set had noticeably shorter ignition delays than the larger nozzles that varied from a 0.05 to 0.2 msec reduction. This observation is expected since the injection velocity was slightly higher for the small nozzle leading to more rapid turbulent shear layer mixing and also due to the fact that smaller nozzles tend to exhibit higher shear layer mixing rates in comparison to large nozzles at a given injection velocity. Also, it is noted that the JP-8 small nozzle data set exhibited an average decrease in the ignition delay by 0.05 msec in comparison to DF-2 small nozzle samples. This small variance is due to the slightly higher injection velocities

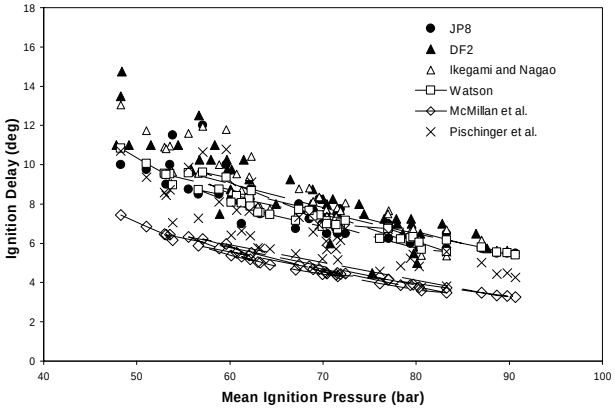


Figure 9: A comparison between AVL 521 JP-8 and DF-2 ignition data utilizing the small nozzle (0.176 mm) and common zero-dimensional ignition models.

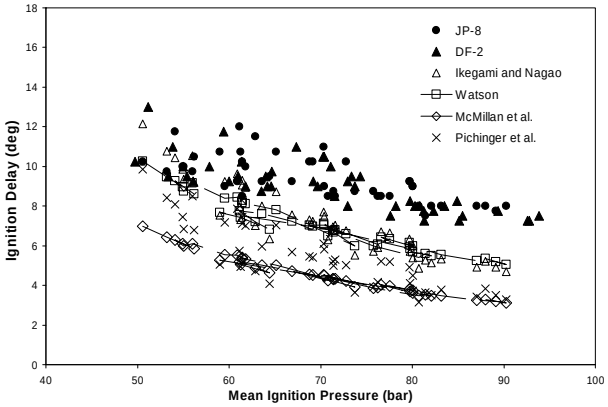


Figure 10: A comparison between AVL 521 JP-8 and DF-2 ignition data utilizing the large nozzle (0.212 mm) and common zero-dimensional ignition models.

associated with JP-8 versus DF-2. Last, the small nozzle ignition delay data set was compared with four common thermodynamic engine cycle simulation ignition models (Ikegami and Nagao, 1969-70; Watson, 1981; Pischinger et al., 1988; McMillan et al., 1983) as given in figure 9. The latter two models yielded large predictive ignition delay errors while the former two showed promise of predicting ignition delay within 25% which is acceptable for cycle simulation modeling purposes. One drawback of such models is their lack of ability to incorporate spray mixing effects since such models are Arrhenius in form (i.e. $P^{-n}$ *exp{E/T}); the correlations that predicted well for the small nozzle data set significantly under-predicted the ignition delay for the large nozzles due to this mixing effect (see figure 10).

### 3.4 Combustion Characteristics

The heat release event in standard diesel combustion includes a rapid pressure rise rate following an ignition delay period that results in a 'spike-like' initial burning profile as a turbulent flame encompasses a portion of the injected fuel jet. Afterward, there is a decrease in the burning rate until the mixing rate exceeds the fuel consumption rate – see figure 1. This particular submission is focused on the premixed phase of combustion ('spike-like initial burning profile).

Past work theorized that the evaporated fuel could be scaled directly to the premixed phase peak combustion rate and also the pressure rise rate if the effective turbulent flame speed rate could be estimated based on characteristic turbulent time scale arguments (Schihl et al., 2006). Since that time, much heat release data has been acquired utilizing the AVL 521 engine and thus a direct comparison has been made between the peak premixed phase combustion rate and the estimated evaporated fuel at the time of ignition. The evaporation rate was estimated assuming that the liquid core is an intact solid right cylinder and that the difference between

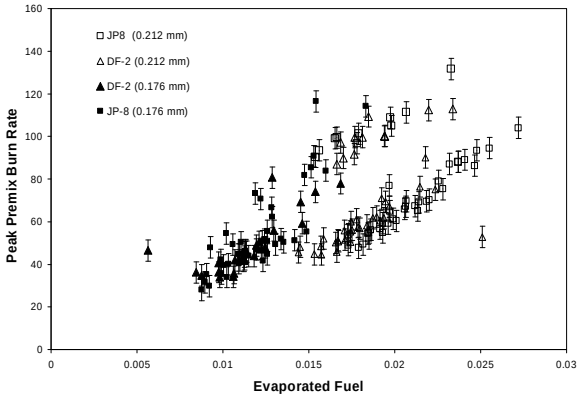


Figure 11: The influence of JP-8 and DF-2 evaporation rate on the peak premixed phase burn rate.

the injected fuel mass during the ignition delay period and intact core volume (and thus mass) is representative of the evaporated fuel at ignition – this relationship is given below:

$$m_{evap} = \int_{t_{SOI}}^{t_{IGN}} \dot{m}_{inj}\, dt - \pi \bullet \frac{d^2}{4} \bullet L_b \qquad \textbf{(5)}$$

and $\dot{m}_{inj}$ is the injection rate, $t_{soi}$ is start of injection time, and $t_{ign}$ is the start of ignition. The net result is shown in figure 11 which demonstrates that the JP-8 and DF-2 peak premixed combustion rate scales linearly with the estimated evaporated fuel for roughly two-hundred data points. Furthermore, it is apparent that the smaller nozzle exhibited higher combustion rates for a similar amount of evaporated fuel in comparison to the large nozzle which is readily explained by the increase in the mixing layer turbulence intensity associated with the smaller nozzle that augments turbulent entrainment into the turbulent flame front. Additionally, both DF-2 and JP-8 evaporated fuel correlated with the peak combustion rate and thus

fuel volatility, given that both fuels had the same cetane number, must be considered in determining the peak pressure rise rate in a diesel engine.

Careful examination of figure 11 also reveals that approximately twenty-five data points exhibited a higher peak premixed burn rate compared to the majority of the data. Most of these points were for the large nozzle and occurred within test matrices A and B where the ratio of peak burning to evaporation rate was highest in comparison to cases C through H, and also where the temperature and pressure at start-of-injection were lowest throughout the text matrix. Additionally, the heat release profiles for these outlaying data points tended to have a peak premixed burning rate larger or comparable to the peak mixing controlled burn rate. There is no conclusive evidence at this point to explain the root cause of the outlaying data points.

## CONCLUSION

Progress to date on improving and quantifying combustion characteristic differences between DF-2 and JP-8 has included (1) the development of a methodology to predict JP-8 evaporation for comparison to DF-2 from a spray targeting viewpoint, (2) an evaluation of potential Arrhenius-type ignition models for JP-8 use, (3) a comparison of cetane number effect on ignition between DF-2 and JP-8, and (4) the impact of vaporization rate on the peak premixed combustion and pressure rise rates. Such comparisons included data taken from a reflection shock tube, a constant volume bomb, a single cylinder research engine, and production multi-cylinder engine. These initial findings will be utilized in the future to develop JP-8 combustion characteristics engineering models including evaporation rate, ignition delay, premixed combustion, and mixing controlled combustion.

## ACKNOWLEDGEMENTS

The authors thank Mr. ‘Mike’ Radic and Ms. Kayla Pence for their efforts in conducting the AVL 521 experiments and post processing in-cylinder pressure measurements.

## REFERENCES

Hardenburg, H.O. and Hase, F.W., 1979, ”An Empirical Formula for Computing the Pressure Rise Delay of a Fuel from its Cetane Number and from Relevant Parameters of Direct-Injection Diesel Engines”, SAE Paper 790493.

Ikegami, M. and Nagao, F., 1969-70, "An Analysis of Combustion Knock in a Diesel Engine", Institution of Mechanical Engineers, **184 (3J)**, 62-66.

Ishiyama, T., Shioji, M., Ihara, T., and Katsuura, A., 2003, “Modeling and Experiments on Ignition of Fuel Sprays Considering the Interaction Between Fuel-Air Mixing and Chemical Reactions”, SAE Paper 2003-01-1071.

Kanimoto, T., Minagawa, T., and Kobori, S., 1997, “A Two-Zone Model Analysis of Heat Release Rate in Diesel Engines”, SAE Paper 972959.

McMillan, M.L., Siegla, D.C., Srinivasan, N., and Tuteja, A.D., 1983, “A Review of GM Investigations of the Effects of Fuel Characteristics on Diesel Engine Combustion and Emissions”, Coordinating Research Council Diesel Fuel Workshop.

Pickett, L.M. and Hoogterp, L., “Fundamental Spray and Combustion Measurements of JP-8 at Diesel Conditions”, SAE Paper 2008-01-1083.

Pischinger, F., Reuter, V., and Scheid, E., 1988, "Self-Ignition of Diesel Sprays and its Dependence on Fuel Properties and Injection Parameters", *Journal of Engineering Gas Turbines and Power*, **110**, 399-404.

Schihl, P., Hoogterp, L., and Pangilinan, H., 2006, “Assessment of JP-8 and DF-2 Evaporation Rate and Cetane Number Differences on a Military Diesel Engine”, SAE Paper 2006-01-1549.

Schihl, P.., Pangilinan, H., and Hoogterp, L., 2008, “Assessment of JP-8 and DF-2 Evaporation Rate and Cetane Number Differences on a Military Diesel Engine”, SAE Paper 2006-01-1549.

Schreiber, M., Sakak, A.S., Lingens, A., and Griffiths, J.F., 1994, “A Reduced Thermokinetic Model for the Autoignition of Fuels with Variable Octane Ratings”, *Twenty-Fifth International Symposium on Combustion*, 993 – 940.

Shipinski, J., Myers, P.S., and Uyehara, O.A., 1969-70, “A Spray Droplet Model for Diesel Combustion”, *Symposium on Diesel Engine Combustion*, Institution of Mechanical Engineers, **184**, 28 - 35.

Siebers, D., 1999, “Scaling Liquid-Phase Penetration in Diesel Sprays Based on Mixing-Limited Vaporization”, SAE Paper 1999-01-0528.

Siebers, D.L., 1985, “Ignition Delay Characteristics of Alternative Diesel Fuels: Implications on Cetane Number”, SAE Paper 852102.

Teng, H., McCandless, J.C., and Schneyer, J.B., 2003, “Compression Ignition Delay of Dimethyl Ether – An Alternative Fuel for Compression-Ignition Engines”, SAE Paper 2003-01-0759.

Vasu, S.S., Davidson, D.F., and Hanson, R.K., 2008, “Jet Fuel Ignition Delay Times: Shock Tube Experiments Over Wide Conditions and Surrogate Model Predictions”, *Combustion and Flame*, **152**, 125-143.

Xia, Y.Q. and Flanagan, R.C., “Ignition Delay – A General Engine/Fuel Model”, SAE Paper 870591, 1987.

Watson, N., 1981, "Transient Performance Simulation and Analysis of Turbocharged Diesel Engines", SAE Paper 810338.